Superoxide Signaling Mediates *N*-acetyl-L-cysteine–Induced G_1 Arrest: Regulatory Role of Cyclin D1 and Manganese Superoxide Dismutase

Sarita G. Menon,[1] Ehab H. Sarsour,[2] Amanda L. Kalen,[2] Sujatha Venkataraman,[2] Michael J. Hitchler,[2] Frederick E. Domann,[2] Larry W. Oberley,[2] and Prabhat C. Goswami[2]

[1]Department of Microbiology and Immunology, State University of New York at Buffalo School of Medicine, Buffalo, New York and [2]Free Radical and Radiation Biology Program, Department of Radiation Oncology, Holden Comprehensive Cancer Center, Iowa City, Iowa

Abstract

Thiol antioxidants, including *N*-acetyl-L-cysteine (NAC), are widely used as modulators of the intracellular redox state. We investigated the hypothesis that NAC-induced reactive oxygen species (ROS) signaling perturbs cellular proliferation by regulating the cell cycle regulatory protein cyclin D1 and the ROS scavenging enzyme Mn–superoxide dismutase (MnSOD). When cultured in media containing NAC, mouse fibroblasts showed G_1 arrest with decreased cyclin D1 protein levels. The absence of a NAC-induced G_1 arrest in fibroblasts overexpressing cyclin D1 (or a nondegradable mutant of cyclin D1-T286A) indicates that cyclin D1 regulates this G_1 arrest. A delayed response to NAC exposure was an increase in both MnSOD protein and activity. NAC-induced G_1 arrest is exacerbated in MnSOD heterozygous fibroblasts. Results from electron spin resonance spectroscopy and flow cytometry measurements of dihydroethidine fluorescence showed an approximately 2-fold to 3-fold increase in the steady-state levels of superoxide ($O_2^{\cdot -}$) in NAC-treated cells compared with control. Scavenging of $O_2^{\cdot -}$ with Tiron reversed the NAC-induced G_1 arrest. These results show that an $O_2^{\cdot -}$ signaling pathway regulates NAC-induced G_1 arrest by decreasing cyclin D1 protein levels and increasing MnSOD activity. [Cancer Res 2007;67(13):6392–9]

Introduction

Thiol antioxidants are well known for their free radical scavenging and antioxidant properties. *N*-acetyl-L-cysteine (NAC), a sulfidryl containing thiol antioxidant, is used in the treatment of acetaminophen-induced hepatotoxicity, immunomodulation in HIV patients, and cardiovascular diseases, for cancer prevention, and as chelating agent in acute heavy metal poisoning (1). NAC is also widely used in basic science research to manipulate a wide variety of oxidation-reduction (redox)–sensitive signaling processes, including inhibiting activation of redox-sensitive transcription factors [nuclear factor κB (NF-κB) and activator protein (AP-1)] and mitogen-activated protein kinase (MAPK) signaling pathways (2–4). Although there is a general assumption that NAC mediates these affects by altering intracellular redox states, the exact mechanism of NAC's action is still not completely understood. Because NAC has a wide application in many areas of medicine and research, a detailed understanding of its mechanism can prove to be very beneficial.

The cellular redox state is a delicate balance between production of prooxidants and antioxidants that scavenge them. Reactive oxygen species (ROS; e.g., superoxide, $O_2^{\cdot -}$) are generated during the four-electron reduction of molecular oxygen to water for energy generation. Superoxide is converted to hydrogen peroxide (H_2O_2) by superoxide dismutase enzymes (MnSOD, CuZnSOD, and ECSOD), whereas catalase and glutathione peroxidase convert H_2O_2 to O_2 and H_2O (5). MnSOD, a nuclear-encoded and mitochondria-localized homotetrameric enzyme, is the primary defense against mitochondrially generated ROS (6). In recent years, it has been shown that ROS generated by cellular metabolism and receptor activation (platelet-derived growth factor and epidermal growth factor) function as "secondary messengers" in numerous signaling pathways governing several cellular processes, including proliferation (7–9).

Cellular proliferation is a highly coordinated event requiring sequential assembly and activation of phase-specific protein kinase complexes, consisting of a cyclin and a cyclin-dependent kinase (CDK; ref. 10). The cyclin-CDK partner first responding to mitogenic signals in G_1 is the cyclin D1/CDK4/6 kinase complex (11). Once activated, the kinase phosphorylates the retinoblastoma protein, releasing the transcription factor E2F that promotes progression from G_1 to S. During late G_1 and S, cyclin D1 is proteasomally degraded after phosphorylation at Thr^{286} by the glycogen synthase kinase GSK-3β (12). Apart from the positive regulators, i.e., cyclin-CDK kinases, the cell cycle has negative regulators known as CDK inhibitors (e.g., p21 and p27) which bind the kinase complexes and prevent their unscheduled activation. Although many of the cell cycle regulatory proteins, like cyclin D1, Cdc25 phosphatase, p21, and retinoblastoma, have been shown to be sensitive to fluctuations in intracellular redox environment (13–18), information about specific regulatory pathways controlling this redox sensitivity is limited.

This study was designed to determine if ROS signaling regulates cell cycle progression after exposure to NAC. Our results show varying doses (5–20 mmol/L) of NAC-induced G_1 arrest in fibroblasts. NAC-induced G_1 arrest is preceded by an increase in the steady-state levels of superoxide radical anion and a decrease in cyclin D1 protein levels. Furthermore, our results show that NAC's "antioxidant" property could be, in part, due to the increased MnSOD activity.

Materials and Methods

Cells and Reagents

NIH3T3-overexpressing cells and NIH3T3 cyclin D1–overexpressing cells were obtained from Dr. Dawn Quelle, University of Iowa. Mouse fibroblasts

Note: Supplementary data for this article are available at Cancer Research Online (http://cancerres.aacrjournals.org/).

Requests for reprints: Prabhat C. Goswami, Free Radical and Radiation Biology Program, Department of Radiation Oncology, B180 Medical Laboratories, University of Iowa, Iowa City, IA 52242. Phone: 319-384-4666; Fax: 319-335-8039; E-mail: prabhat-goswami@uiowa.edu.

doi:10.1158/0008-5472.CAN-07-0225

with MnSOD wild type and heterozygous were a kind gift from Dr. Ting-Ting Huang, Stanford University. Normal human skin fibroblasts were purchased from American Type Culture Collection. All cells were maintained in DMEM (Life Technologies) supplemented with 10% heat-inactivated fetal bovine serum (FBS; HyClone Laboratories) and antibiotics (penicillin and streptomycin). NIH3T3 Flag D1 T286A cells, graciously provided by Dr. Alan Diehl, University of Pennsylvania, were maintained in DMEM supplemented with 10% FBS, glutamine, antibiotics, and puromycin (7.5 μg/mL; BD Biosciences). All cells were cultured at 37°C in a humidified incubator with 5% CO_2 and 95% air. Adenoviruses overexpressing human catalase cDNA (Ad*CAT*) and antibodies to MnSOD were obtained from The University of Iowa Gene Transfer Vector Core and Radiation and Free Radical Research Core. Anticyclin D1 mouse monoclonal antibodies were purchased from PharMingen. Tiron (4,5-dihydroxy-1,3-benzenedisulfonic acid disodium salt) and catalase protein were purchased from Sigma. NAC was prepared as 1 mol/L of stock solutions with sodium bicarbonate and pH of 7.0. To prevent oxidation, NAC stocks were prepared fresh just before addition to the culture.

Flow Cytometry Assays

Propidium iodide staining for DNA content measurement. Monolayer cultures, trypsinized and fixed in 70% ethanol, were washed once with PBS and treated with RNase A for 30 min, followed by staining with propidium iodide (PI; 35 μg/mL); and DNA content was measured using flow cytometry. Percentage of cells in each phase of the cell cycle was analyzed using MODFIT software.

Bromodeoxyuridine pulse and pulse-chase assays. Asynchronously growing cells were pulse labeled with 10 μmol/L bromodeoxyuridine (BrdUrd; Sigma) for 30 min at 37°C. In a BrdUrd pulse assay, cells were harvested and ethanol fixed; in a BrdUrd pulse-chase assay, cells were continued in BrdUrd-free culture medium containing thymidine and cytidine (10 μmol/L each). Cells were harvested at representative time points by trypsinization, fixed in 70% ethanol, and stored at 4°C. Ethanol-fixed cells were washed with PBS + 0.1% Tween 20 (PBT) and incubated in Pepsin-HCl (0.3 mg pepsin/mL 2N HCl). Isolated nuclei were incubated for 1 h at room temperature with anti-BrdUrd antibody (Becton Dickinson Immunocytometry Systems) followed by incubation with FITC-conjugated goat anti-mouse IgG secondary antibody. Nuclei were then washed with PBT, incubated with RNase A, PI (35 μg/mL), and analyzed by flow cytometry. Histograms were displayed as dual variable: PI (DNA content) versus log FITC. Data was collected from 20,000 nuclei and DNA content was analyzed using the Cell Quest software as previously described (14–16).

Immunoblotting

Cells were collected by scrape harvesting and pelleted by centrifugation. Total protein extracts were prepared by sonication, and protein concentrations were determined by Bradford assay. Equal amounts of protein were electrophoresed in a 12.5% SDS-polyacrylamide gel and transferred onto a nitrocellulose membrane (Protran, Schleicher & Schuell) and blocked with 5% nonfat dry milk for 1 h. Blots were washed thrice with 0.1 mol/L Tris-HCl (pH 7.5), 0.15 mol/L NaCl, and 0.1% Tween 20 (TBST) and incubated with primary antibodies at 4°C. The blots were washed with TBST and incubated with secondary antibodies for 1 h at room temperature. Immunoreactive bands were detected using horseradish peroxidase–conjugated secondary antibodies and enhanced chemiluminescence detection reagents (Amersham). The bands were visualized and quantitated with a computerized digital imaging system using AlphaImager 2000 software. Actin protein levels were used for loading controls, and fold change calculated relative to untreated control.

Real Time PCR Analysis

Total cellular RNA was isolated using Trizol reagent (Invitrogen). Using Superscript III RNase H-reverse transcriptase kit (Invitrogen), cDNA was synthesized with 5 μg RNA and random hexamers. PCR primers for MnSOD, cyclin D1, and 18S (endogenous control) were designed using Primer Express 2.0 (Applied Biosystems). Primers were designed across exon boundaries to ensure no genomic DNA was amplified: cyclin D1: forward 5′-GCTGCTGCAAATGGA ACTGCT-3′ and reverse 5′-CATCCGCCTCTGGCATTTT-3′; MnSOD, forward 5′-CCACACATTAACGCGCAGATC-3′ and reverse 5′-TAACATCTCCCTT GGCCAGAGC-3′; 18S, forward 5′-GCCCGAAGCGTTTACTTTGA-3′ and reverse 5′-TCATGGCCTCAGTTCCGAA-3′. Real-time PCR assay was done using SYBR Green PCR Mastermix (Applied Biosystems): 0.5 ng/μL of reverse transcribed cDNA and 5 μmol/L each of forward and reverse primers. The PCR amplification was done in an ABI 7000 thermal cycler using the absolute quantification method. Cycle threshold (Ct), which is the number of cycles required to reach the linear range of fluorescence intensity, was calculated from each sample with the ABI Prism 7000 Sequence Detection Software. A Ct value calculated from samples in triplicates was averaged, and relative mRNA levels of cyclin D1 and MnSOD were calculated using the formula ΔCt = Ct (cyclin D1 or MnSOD)/Ct (18S).

Antioxidant Enzyme Activity Assays

Biochemical measurements of MnSOD and CuZnSOD enzyme activities were determined according to the nitroblue tetrazolium-bathocuproinedisulfonic acid (NBT-BCS) superoxide dismutase assay (19). Activities between CuZnSOD and MnSOD were distinguished by differential sensitivity to sodium cyanide. Catalase activity was determined spectrophotometrically at 240 nm by following the disappearance of 10 mmol/L hydrogen peroxide in 50 mmol/L potassium phosphate (pH 7.0; ref. 20).

Dihydroethidine Assay

Dihydroethidine was used to measure superoxide levels. Cells were washed with PBS and labeled with 10 μmol/L dihydroethidine (in 1% DMSO) for 40 min at 37°C. Cells were trypsinized with phenol-free trypsin/EDTA on ice. Trypsin was inactivated with media containing 10% FBS. Cells were collected and resuspended in PBS. Samples were analyzed using flow cytometry (excitation, 488 nm; emission, 585 nm). Mean fluorescence intensity was analyzed using CellQuest software. Samples were corrected for autofluorescence using unlabeled cells. Antimycin A (10 μmol/L in 1% DMSO) was used as positive control.

Electron Spin Resonance Spectroscopy

5,5-dimethyl-1-pyrroline N-oxide (DMPO) was the spin trap used to detect free radical production. Electron spin resonance (ESR) measurements were made using a Bruker EMX 300 spectrometer with a magnetic field modulation frequency of 100 kHz and microwave power of 40 mW. The scans were traced with modulation amplitude of 1 G, scan rate of 80 G/81 s, and receiver gain of 10^4 to 10^6. Fibroblasts treated with NAC (20 mmol/L) for 45 min were rinsed with PBS and covered with 500 μL of chelated PBS (iminodiacetic acid, sodium form, dry mesh 50–100; Sigma) containing DMPO (100 mmol/L). Cells were then incubated at 37°C for 15 min, scraped, and transferred to a flat cell for ESR measurement. Specificity of the $O_2^{\bullet-}$ signal was determined by preincubating the monolayer cells with CuZnSOD (1000 units) or Tiron (1 mmol/L) followed by the addition of DMPO. ESR peak heights were calculated and normalized to 1×10^6 cells (21).

Adenovirus Gene Transfer

Fibroblasts were plated in complete medium and were allowed to attach for 24 h. Cells were infected with adenovirus (30–50 multiplicity of infection) in serum-free media for 24 h; the adenoviruses contained human *catalase* cDNA (Ad*CAT*). Serum-free media were replaced with serum-containing media, and cells continued in culture for another 24 h before adding NAC. An unaltered vector (Ad*Bgl II*) was used as a control (16, 22).

Statistical Analysis

Data are presented as means ± SD from at least three independent experiments. Statistical significance of data was evaluated using Student's *t* test and one-way or two-way ANOVA. Results were considered statistically significant at $P < 0.05$. All Western blots were done at least twice to show reproducibility.

Results

A NAC-induced G_1 arrest is associated with decrease in cyclin D1 and increase in MnSOD protein levels. To determine if exposure to NAC perturbs cell cycle progression, exponentially

growing asynchronous cultures of NIH3T3 mouse fibroblasts were cultured in a medium containing varying doses of NAC (5–20 mmol/L) for 24 h. In a separate series of experiments, cells were treated with 20 mmol/L NAC for 24 h and stained with PI for flow cytometry measurement of cell viability. Results showed majority of the cells (>95%) were viable during the course of the experiment (Supplementary Fig. S3). NAC-treated cells were pulse labeled for 30 min with BrdUrd, a thymidine analogue used for labeling S-phase cells. Figure 1*A* is a representative histogram of 3T3 cells showing the distribution of cells in G_1, S, and G_2 in the absence and presence of NAC (20 mmol/L). NAC exposures showed a dose-dependent increase in the percentage of G_1 cells ($\sim$90% in 20 mmol/L NAC-treated cells) with a concomitant reduction in percentage of S-phase cells (Supplementary Table S1).

To determine if NAC-induced perturbations in cellular proliferation were specific to a cell cycle phase, a BrdUrd pulse-chase assay was used to measure transit times of each cell cycle phase. Control cells transit G_1 with a median transit time of 12 h, whereas the NAC-treated population still showed $\sim$80% cells in G_1 at 12 h, indicating a G_1 arrest (Supplementary Fig. S1*B*). Measurement of relative movement, indicative of S-phase transit time (23), showed that NAC did not affect transit through S phase (Supplementary Fig. S1*C*). Likewise, measurements of BrdUrd-positive cells that completed cell division (G_1^+ fraction) did not show any difference between untreated and NAC-treated cells, indicating transit through S and G_2 + M were unaffected (Supplementary Fig. S1*D*). These results show that NAC-induced cell cycle perturbation was specific to the G_1 phase of the cell cycle.

To determine if NAC-induced regulation of G_1 to S transition is associated with changes in cyclin D1 protein levels, lysates from both control and NAC-treated cells were collected after 24 h and used for Western blot analysis. Cyclin D1 protein levels showed a dose-dependent decrease to 10% in cells treated with 20 mmol/L NAC (Fig. 1*B*). Furthermore, exposure to NAC caused an increase in the antioxidant protein MnSOD, 1.8-fold in 5 mmol/L and 3.9-fold in 20 mmol/L NAC-treated cells (Fig. 1*C*). Interestingly, this increase in MnSOD protein levels seems to be a late effect of NAC exposure and was seen only after almost 24 h of exposure to 20 mmol/L NAC (Fig. 1*D*). Based on these observations it seems both cyclin D1 and MnSOD play an important role in mediating the NAC-induced G_1 arrest.

NAC-induced G_1 arrest is dependent upon cyclin D1 protein levels. Because NAC induced a dose-dependent decrease in cyclin D1 protein levels (Fig. 1*B*), we determined if this decrease was dependent upon the duration of NAC exposure. A NAC-induced decrease in cyclin D1 protein levels occurred as early as 4 h into NAC treatment (50% decrease; Fig. 2*A*), which preceded decrease in S-phase fraction (Fig. 2*C*). To shed light on the role of cyclin D1 in mediating the NAC-induced G_1-arrest, NAC's effect on cellular progression from quiescence (G_0) to G_1 to S was examined. Exponentially growing 3T3 fibroblasts were serum starved and recruited to the G_0 phase of the cycle. Cells were then serum stimulated to reenter the cell cycle in the presence and absence of 20 mmol/L NAC and harvested at fixed time intervals for immunoblotting and cell cycle analysis. In control cells reentering the cell cycle, cyclin D1 protein levels begin to increase between 8 and 10 h. In contrast, cells cultured in presence of NAC did not show any increase in cyclin D1 even after 10 to 12 h of serum stimulation (Fig. 2*B*).

To examine if a NAC-induced decrease in cyclin D1 was associated with corresponding changes in its mRNA levels, quantitative real-time PCR analysis was used. Total cellular RNA from exponential 3T3 cultures treated with different concentrations of NAC (0–20 mmol/L) were reverse transcribed, and the cDNA obtained was then subjected to real-time PCR assay for simultaneous amplification of mouse *cyclin D1* and *18S* mRNA. There was no change in *cyclin D1* mRNA levels with NAC treatment (Fig. 2*D*). These results suggest that the decrease in cyclin D1 levels after NAC exposure was not a transcriptional response.

To determine if cyclin D1 regulates NAC-induced G_1 arrest, 3T3 parental cells stably overexpressing cyclin D1 (3T3D1) were cultured in the presence and absence of 20 mmol/L NAC for

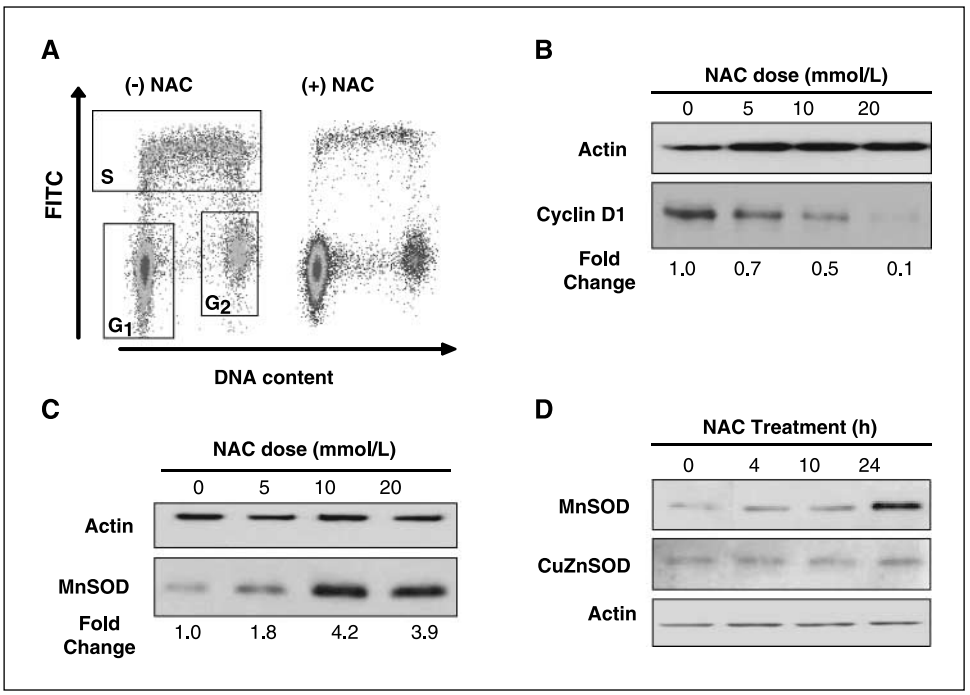

Figure 1. Thiol antioxidant–induced G_1 arrest is associated with decreased cyclin D1 and increased MnSOD protein levels. *A,* exponentially growing NIH3T3 fibroblasts were treated with 0, 5, 10, and 20 mmol/L NAC for 24 h. Cell cycle phase distribution was measured using BrdUrd pulse and dual variable flow cytometry assay. Representative FITC-PI histograms of cell cycle phase distributions in control and 24 h after exposure to 20 mmol/L NAC. Percentage of cell cycle phase distributions is presented in Supplementary Table S1. Western blot analysis of cyclin D1 (*B*) and MnSOD (*C*) protein levels after 24 h of treatment with NAC. *D,* immunoblot analysis of MnSOD protein levels from lysates treated with 20 mmol/L NAC for 4, 10, and 24 h. Blots were scanned and quantitated using Alphalmager; actin levels were used for loading control. Fold change was calculated by first normalizing to actin levels in individual samples and then relative to untreated control.

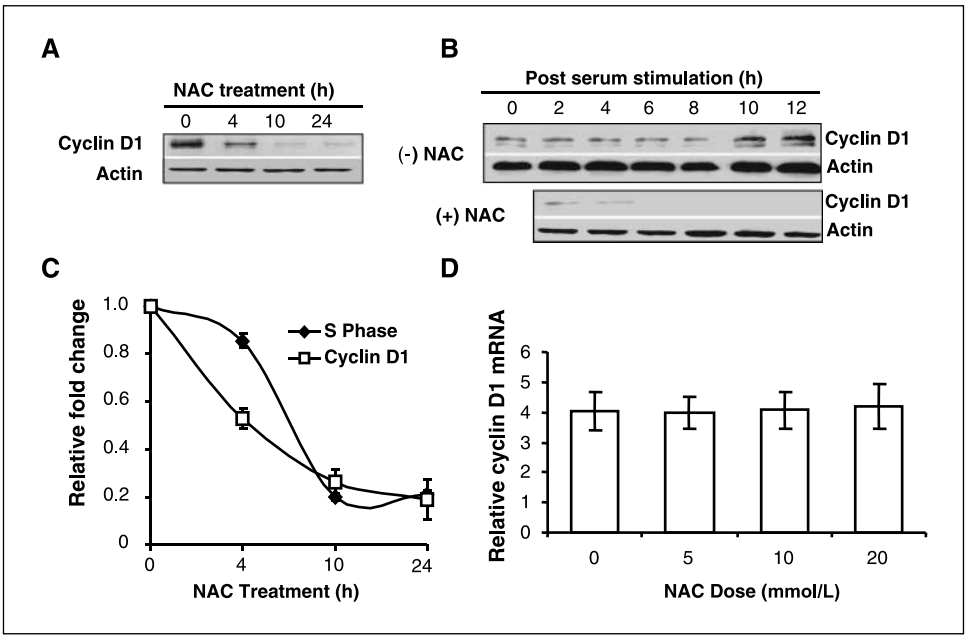

Figure 2. Thiol antioxidant–mediated decrease in cyclin D1 protein levels is independent of changes in its mRNA levels. *A,* time course of NAC-induced decrease in cyclin D1 protein levels in 3T3 cells treated with 20 mmol/L NAC. *B,* effect of NAC on cyclin D1 protein levels in 3T3 cells entering cell cycle from density-arrested G_0 phase. Western blot analysis of cyclin D1 in the presence and absence of 20 mmol/L NAC harvested at various time intervals after serum stimulation. *C,* quantitative representations of relative fold change in cyclin D1 protein and S-phase distribution in cells exposed to 20 mmol/L NAC for different intervals of time. *D,* real-time PCR analysis of cyclin D1 mRNA levels in 3T3 fibroblasts treated with NAC (0–20 mmol/L). 18S RNA was amplified as internal control, and relative cyclin D1 levels in each sample were calculated by normalizing to its corresponding 18S RNA level ($n = 3$).

24 h. Cells were then pulse labeled with BrdUrd and assayed for cell cycle phase distribution using flow cytometry (Fig. 3*A*). Exponential untreated 3T3 parental cultures showed a cell cycle distribution of 60% in G_1, 28% in S, and 10% in G_2. Upon NAC treatment, there was a significant increase in G_1 phase (86%) and a concomitant decrease in S phase to 6%. However, NAC exposure caused only a minimal change in cell cycle redistribution in 3T3D1 cells. 3T3D1 cells had 47% cells in G_1 phase, 38% S, and 12% G_2, and NAC exposure resulted in redistribution with 59% G_1, 29% S, and 9% G_2. The small increase in G_1 could be due to a fraction of cyclin D1 still being degraded after NAC exposure (Fig. 3*B*). Therefore, these experiments were repeated in 3T3 cells expressing a nondegradable cyclin D1-T286A mutant. The cyclin D1-T286A mutant cannot be phosphorylated by GSK-3β and therefore is stabilized in the cell. The cyclin D1-T286A mutant cell line was resistant to a NAC-induced G_1 arrest; the S-phase fractions were ~51% in untreated cells and did not show any significant reduction (47%) after 24 h of NAC exposure (Fig. 3*A*). Likewise, NAC exposure did not cause any changes in cyclin D1 protein levels compared with control (Fig. 3*C*). These results strongly suggest that cyclin D1 regulates the NAC-induced G_1 arrest.

Increase in MnSOD activity is a delayed response to NAC exposure. We investigated if the NAC-induced increase in MnSOD protein levels (Fig. 1*C*) was also associated with increased MnSOD activity. 3T3 cells were exposed to NAC for various periods of time; MnSOD activity was then measured by the NBT-BCS superoxide dismutase biochemical activity assay (19). MnSOD activity showed a concomitant increase from 1.5-fold at 4 h to ~3.5-fold at

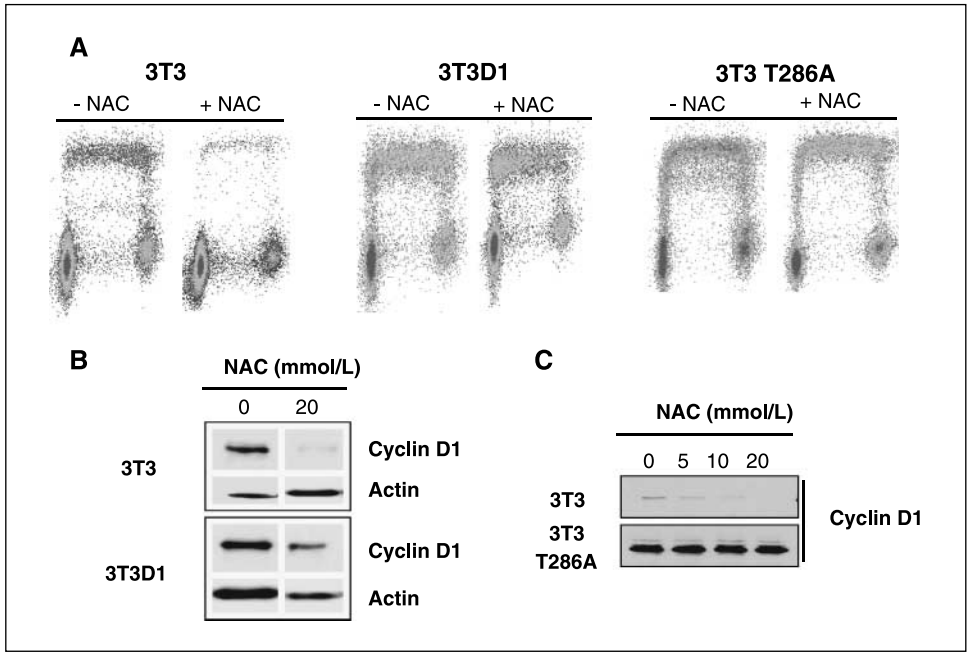

Figure 3. Regulatory role of cyclin D1 in mediating NAC-induced G_1 arrest. *A,* histograms from flow cytometric BrdUrd-PI assay of NAC-treated (20 mmol/L) and untreated 3T3 fibroblasts (*left*), Cyclin D1-overexpressing cells 3T3D1 (*center*), and cells expressing a Flag tagged cyclin D1 nondegradable mutant D1-T286A (*right*). *B,* Western blot analysis of cyclin D1 protein levels in 3T3 and 3T3D1 cells in the presence and absence of 20 mmol/L NAC. *C,* immunoblot analysis of cyclin D1 protein levels in wild-type 3T3 cells and 3T3 cells expressing flag-tagged cyclin D1-T286A treated with NAC (0–20 mmol/L).

24 h (Fig. 4*A*). Furthermore, increase in MnSOD activity correlated inversely with a decrease in S phase (38% at 4 h to 7% at 24 h). Catalase activity showed ~2-fold increase after 24 h of NAC exposure. However, there was no significant change in CuZnSOD activity in NAC-treated cells compared with untreated control.

Quantitative PCR assay was used to measure *MnSOD* mRNA levels from cells exposed to 5, 10, and 20 mmol/L NAC for 24 h. *MnSOD* mRNA levels were first normalized to individual 18 S mRNA levels, and relative fold-change was calculated relative to untreated control (0 mmol/L). Results presented in Fig. 4*B* showed no difference in *MnSOD* mRNA levels in fibroblasts cultured in the presence of 5, 10, and 20 mmol/L NAC. These results show that

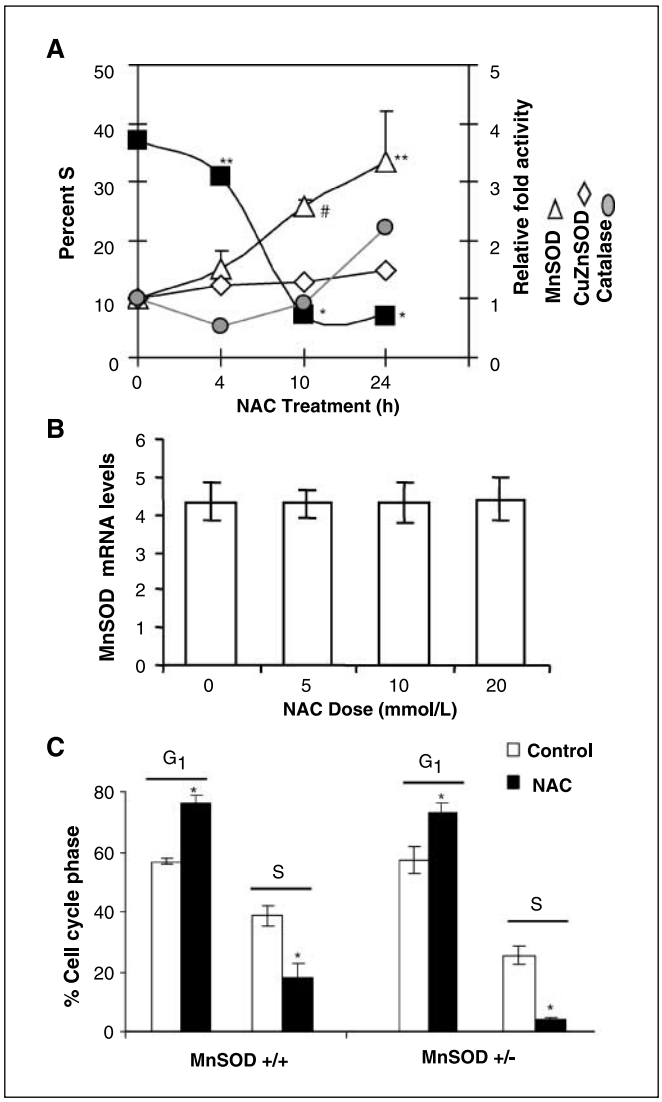

Figure 4. NAC-induced MnSOD activity aides in regulating G_1 arrest. *A,* exponentially growing 3T3 cells treated with 20 mmol/L NAC were collected at different intervals and assayed for enzymatic activity of MnSOD, CuZnSOD, and catalase. Relative activity of each enzyme plotted and compared with changes in percentage of S phase. *, $P < 0.001$; **, $P < 0.01$; #, $P < 0.05$ versus 0 h. *B,* real-time quantitative PCR analysis of *MnSOD* mRNA levels from samples treated with different doses of NAC (0–20mmol/L) for 24 h. 18S mRNA levels were used for internal control. Quantitation of MnSOD mRNA was done by normalizing to 18S mRNA levels in individual samples; $n = 3$. *C,* mouse fibroblasts with wild-type and heterozygous MnSOD were exposed to 20 mmol/L NAC for 24 h and collected for PI staining and flow cytometry analysis of cell cycle phase distribution.

NAC-induced increases in MnSOD protein and activity were independent of its mRNA levels. Furthermore, protein levels and activity of MnSOD were maximally induced by 24 h of NAC treatment, suggesting MnSOD induction is a delayed response to NAC-mediated alteration in cellular redox environment.

To further determine the regulatory role of MnSOD during NAC-induced G_1 arrest, cell cycle phase distributions were measured in normal mouse fibroblasts carrying wild-type and heterozygous *MnSOD* genotypes. Exponential cultures were incubated with 20 mmol/L NAC for 24 h and fixed in ethanol for flow cytometry analysis of cell cycle phase distributions. Similar to 3T3 cells (Fig. 1*A*), MnSOD wild-type and heterozygous fibroblasts showed a decrease in S-phase cells upon treatment with NAC compared with untreated control cells (Fig. 4*C*). The percentage of S phase in wild-type cells showed ~2-fold decrease in NAC-treated cells compared with control; percentage of S-phase in MnSOD heterozygous fibroblasts decreased ~6-fold in NAC-treated cells compared with control. Accordingly, the percentage of G_1 cells increased in NAC-treated cells compared with controls. Cells in G_2 phase did not change after NAC exposure (data not shown). The increased fold reduction in S phase in MnSOD heterozygous cells compared with wild-type cells strongly suggests that MnSOD has a regulatory role in NAC-induced decrease in S-phase cells.

NAC-induced superoxide signaling regulates G_1 arrest. MnSOD converts superoxide to hydrogen peroxide. Therefore, increases in MnSOD activity in NAC-treated cells suggest that NAC exposures could perturb cellular superoxide levels. An ESR assay was applied to measure the steady-state levels of $O_2^{\bullet -}$ in untreated cells and at the end of 1 h of NAC (20 mmol/L) exposure. Results showed that NAC exposure increased the steady-state levels of $O_2^{\bullet -}$ by ~2-fold (Fig. 5*A* and *B*). The specificity of the assay for measurements of superoxide levels was verified by pretreating the cells with CuZnSOD. CuZnSOD pretreatment suppressed NAC-induced increase in superoxide levels, indicating that ESR signals were specific to $O_2^{\bullet -}$. NAC-induced increase in cellular superoxide levels was further verified by using flow cytometry measurement of dihydroethidine fluorescence. Results presented in Fig. 5*C* showed increase in dihydroethidine fluorescence in cells treated with 20 mmol/L NAC for 1 h compared with control. Dihydroethidine fluorescence subsequently dropped to control levels at 24 h of NAC exposure (data not shown), which correlated to increase in MnSOD activity (Fig. 4*A*). These results clearly show that NAC exposure increased the steady-state $O_2^{\bullet -}$ levels. Cells responded to this increase in superoxide levels by increasing MnSOD activity.

Increase in MnSOD activity corresponded to an increase in hydrogen peroxide levels (Supplementary Fig. S2*A*). Because higher levels of H_2O_2 are growth inhibitory, we determined whether H_2O_2 could play a role in regulating NAC-induced G_1 arrest. 3T3 fibroblasts were transduced with peroxide scavenging enzyme (Ad*CAT*). Transduced cells were then treated with 20 mmol/L NAC, and cell cycle phase distribution was measured by flow cytometry. In a separate set of experiments, catalase (1000 units/mL) was added to cell culture media followed by the NAC addition. Results presented in Supplementary Fig. S2*C* showed that the catalase did not reverse a NAC-induced decrease in the S phase. Likewise, the percentage of G_1 cells remained higher in cells overexpressing catalase and catalase added to the medium before NAC exposure. These results suggest that H_2O_2 might not regulate NAC-induced G_1 arrest and the subsequent decrease in S-phase.

Superoxide scavenging abrogates NAC-induced G_1 arrest. To determine if NAC-induced increase in $O_2^{\bullet -}$ levels regulates G_1

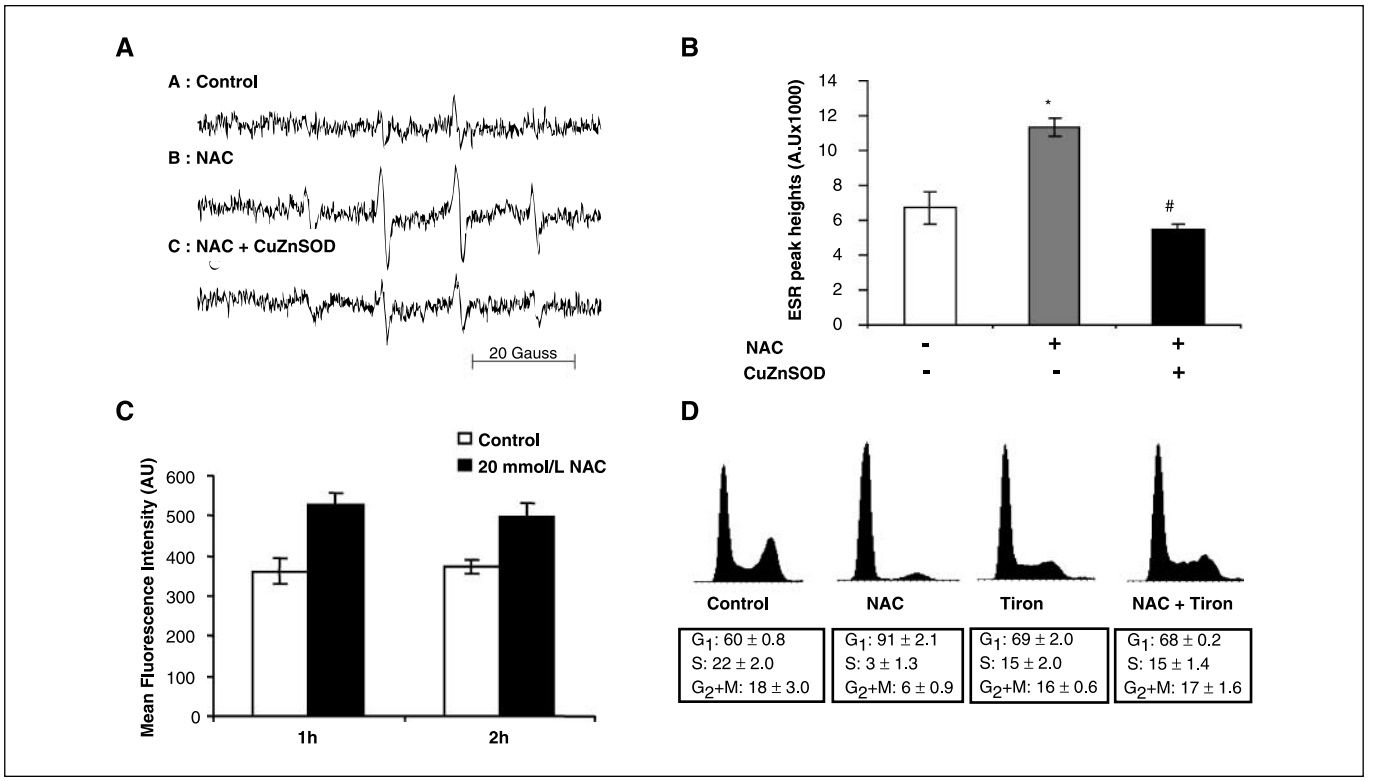

Figure 5. Thiol antioxidant increases steady-state levels of $O_2^{\bullet -}$. *A,* representative ESR spectra of superoxide radical anion. 3T3 fibroblasts were incubated with 20 mmol/L NAC for 45 min, and media was removed. Cells were then incubated with 100 mmol/L of the spin trap DMPO in the presence and absence of 1,000 units of CuZnSOD for 15 min. *B,* ESR peak height. *Columns,* mean of ESR peak height; *bars,* SD ($n = 4$). *, $P < 0.05$ versus control; #, $P < 0.05$ versus 20 mmol/L NAC; *C*, dihydroethidine assay to detect superoxide levels in the cells. After incubation with 20 mmol/L NAC, dihydroethidine is added to the cells at a concentration of 10 μmol/L (in 1% DMSO) for 40 min at 37°C. Cells were then trypsinized, washed with PBS, and analyzed using flow cytometry ($n = 3$). *D,* representative DNA histograms of 3T3 cells treated with 1 mmol/L Tiron and incubated with 20 mmol/L NAC for 24 h. *Columns,* mean; *bars,* SD ($n = 3$); *, $P < 0.05$.

arrest, exponentially growing 3T3 cells were preincubated with a well-known $O_2^{\bullet -}$ scavenger, Tiron (1 mmol/L). NAC (20 mmol/L) was added to the cultures for 24 h. ESR results showed that Tiron reduced the NAC-induced superoxide levels by ~3-fold (data not shown). Consistent with reduction in superoxide levels, pretreatment with Tiron also reversed NAC-induced G_1 arrest; percentage of G_1 decreased from 91% in NAC-treated cells to 68% in NAC and Tiron-treated cells (Fig. 5*D*). Likewise, prior treatment with Tiron reversed NAC-induced decrease in cyclin D1 protein levels (Supplementary Fig. S4). These results show that NAC-induced $O_2^{\bullet -}$ signaling leads to a G_1 arrest by decreasing cyclin D1 and increasing MnSOD activity.

Discussion

Our earlier study (15) and the results presented here show that NAC exposures specifically inhibited progression from G_1 to S in normal fibroblasts. The results of a ROS signaling regulating cell cycle phase transitions are consistent with our earlier work and results from other laboratories (24–26). We have shown previously that the oxidation of a prooxidant-sensitive dye increased in late S and G_2 + M phases of the HeLa cell cycle compared with G_1 (25). Intracellular redox state measured by cellular reduced glutathione (GSH) content varied in each phase of the HeLa and Chinese hamster ovary fibroblasts cell cycles (24, 26). In fact, the concept of redox-sensitive pathways regulating cellular proliferation dates back to 1931 when Rapkine first reported that the levels of soluble thiols in sea urchin eggs reduced until metaphase and then increased toward mitosis (27). ROS (specifically $O_2^{\bullet -}$ and H_2O_2) generated from biochemical redox reactions could modify protein functions via intramolecular or intermolecular disulfide exchange reactions, e.g., H_2O_2 mediated oxidation of cysteines from reduced-SH to oxidized -S-S- form and $O_2^{\bullet -}$ influencing redox state of metal cofactors in kinases and phosphatases. Redox modulations of kinases and phosphatases could influence activities of cell cycle regulatory pathways, which in turn could regulate progression from one cell cycle phase to the next (28).

Recent evidence suggests ROS levels could influence multiple cellular processes, including cellular proliferation (8, 29). However, the precise molecular signaling events of such a regulation are not yet well characterized. We have previously shown treatment of fibroblasts with 20 mmol/L NAC increased intracellular small molecular weight thiols: GSH (11.6 versus 3.3 nmol/mg protein in control), cysteine (2.6 versus 0.67 nmol/mg protein), and NAC (9.4 nmol/mg protein). However, increased thiol pools did not seem to regulate G_1 arrest because inhibition of GSH synthesis using buthionine-(*S, R*)-sulfoximine in NAC-treated cells did not reverse the arrest (15). These earlier results suggest that mechanisms other than cellular thiol pools regulate NAC-induced G_1 arrest. Our current results showed that NAC exposures increased ROS ($O_2^{\bullet -}$) levels in fibroblasts. Because $O_2^{\bullet -}$ is converted into H_2O_2 both spontaneously and enzymatically by superoxide dismutase, it is possible that H_2O_2 could regulate NAC-induced G_1 arrest. This hypothesis is also supported by increases in catalase activity at 24 h of NAC exposure (Fig. 4*A*). Increases in catalase activity are

anticipated to neutralize excess H_2O_2, thereby maintaining a redox balance within cells. However, addition of catalase to the growth medium or overexpression of catalase before NAC exposure did not affect NAC-induced G_1 arrest. These results suggest that H_2O_2-signaling pathways might not regulate G_1 arrest in NAC-treated fibroblasts. Instead $O_2^{\bullet -}$-signaling pathway could mediate NAC-induced G_1 arrest.

NAC-induced increase in cellular $O_2^{\bullet -}$ levels was associated with a decrease in cyclin D1 protein levels. Cyclin D1 is believed to be the first cell cycle protein that responds to mitogenic signals, and ROS are involved during mitogenic signaling of cellular proliferation. Therefore, it is logical to postulate that NAC-induced change in $O_2^{\bullet -}$ levels that occurred within 1 h of treatment is the signaling molecule, and cyclin D1, wherein levels reduced within 2 to 4 h, is the immediate downstream target. Cyclin D1 responds to changes in cellular redox environment by modulating G_1 progression. Evaluation of the exact mechanism by which $O_2^{\bullet -}$ levels could affect cyclin D1 needs additional studies. However, it is reasonable to postulate that redox regulation of cyclin D1 expression could be regulated by the redox-sensitive transcriptional response of the cyclic AMP response element binding protein, NF-κB, AP-1, or Sp1, binding to the promoter region of cyclin D1 (30–32). Therefore, we examined if NAC exposure altered *cyclin D1* mRNA levels, which resulted in decreased cyclin D1 protein levels. Results from real-time PCR assays showed no change in steady-state levels of *cyclin D1* mRNA levels in NAC-treated cells compared with controls, suggesting NAC exposures did not alter *cyclin D1* transcription in 3T3 fibroblasts (Fig. 2*D*).

The cyclin D1 protein contains two phosphorylation sites on residues T286 and T288, which regulate its degradation (12, 33). During late G_1, cyclin D1 is proteasomally degraded after phosphorylation at T286 by GSK-3β (12). Our results show increased expression of cyclin D1 (overexpressed 3T3D1 or a nondegradable mutant 3T3T286A) abrogated a NAC-induced G_1 arrest. Although 3T3D1 overexpressing cells showed some decrease in cyclin D1 protein levels with NAC exposure, levels in the nondegradable mutant T286A did not change. Since the T288 residue was still available for degradation and NAC treatment did not change cyclin D1 protein levels in T286A mutant cells, we conclude phosphorylation at T288 might not be the target for NAC-induced modification. These results strongly suggest the presence of a redox-sensitive pathway that could regulate T286 phosphorylation and cyclin D1 degradation in NAC-treated cells.

In addition to reduction in cyclin D1 levels as an early response to NAC-exposures, a late response to NAC exposures was the increase in MnSOD protein levels and activity. This late response of MnSOD could be due to cellular responses to NAC-induced increase in superoxide levels resulting in G_1 arrest. This is consistent with the observation that cells with lower levels of MnSOD, and thereby possessing a reduced capacity to dismute the superoxide, displayed enhanced G_1 arrest (Fig. 4*C*). These results further suggest NAC-induced superoxide signaling could regulate G_1 arrest. NAC-induced increase in MnSOD protein levels was independent of changes in *MnSOD* mRNA levels (Fig. 4*B*) suggesting that a translational/posttranslational pathway could regulate MnSOD protein and activity in NAC-treated fibroblasts. This hypothesis is consistent with recent reports of posttranslational modifications of catalase and glutathione peroxidase activity via phosphorylation/dephosphorylation modifications (34, 35). NAC exposures selectively increased MnSOD activities without altering CuZnSOD activity. Furthermore, in MnSOD heterozygous fibroblasts NAC-induced decrease in S phase was exacerbated (Fig. 4*C*). The hypothesis of an $O_2^{\bullet -}$-signaling pathway regulating NAC-induced G_1 arrest was further evident from experiments in which Tiron was used to scavenge $O_2^{\bullet -}$. Scavenging of NAC-generated $O_2^{\bullet -}$ with Tiron reversed the G_1 arrest, which was accompanied with a corresponding increase in S-phase percentage (Fig. 5*D*). These results strongly suggest that $O_2^{\bullet -}$-mediated signaling pathways possibly generated from mitochondria regulate NAC's cytostatic effects.

Although the mechanisms generating NAC-induced $O_2^{\bullet -}$ in our experimental system were not investigated, Wlodek (36) proposed that under physiologic conditions, thiols, such as NAC, could undergo one electron oxidation to generate thiyl radicals (RS•). These radicals can react with the thiolate anion (RS^-) form of NAC to form the disulfide radical anion ($RSSR^{\bullet -}$) as an intermediate. In the presence of molecular oxygen, this intermediate disulfide radical anion yields disulfides (RSSR) and the $O_2^{\bullet -}$ radical anion. Such a mechanism could explain the NAC-induced $O_2^{\bullet -}$ generation in our experiments.

NAC has been previously shown to function as a thiol antioxidant by acting on redox-sensitive transcription factors (NF-κB and AP-1) and MAPK signaling pathways (2–4). Whereas most studies that report NAC as a thiol antioxidant have looked at time points around 24 h and beyond, our results indicate that the immediate effect of NAC could be prooxidant (within 1 h), which is subsequently followed by its antioxidant property presumably via activation of MnSOD activity.

In summary, there seems to be a temporal effect of NAC's action on cells, whereby increase in superoxide levels is the immediate response leading to cyclin D1–mediated G_1 arrest. Subsequent to the increase in superoxide levels and G_1 arrest, NAC exposure causes a late effect, increasing MnSOD activity.

Acknowledgments

Received 1/18/2007; revised 4/6/2007; accepted 5/1/2007.

Grant support: NIH CA111365 (P.C. Goswami), University of Iowa Carver Trust (P.C. Goswami), CA66081 (L.W. Oberley), and CA73612 (F.E. Domann).

The costs of publication of this article were defrayed in part by the payment of page charges. This article must therefore be hereby marked *advertisement* in accordance with 18 U.S.C. Section 1734 solely to indicate this fact.

We thank Dr. Garry R. Buettner for assistance with ESR spectroscopy, Justin Fishbaugh (University of Iowa, Flow Cytometry facility) for assisting with the flow cytometry assays, and Kellie Bodeker with editorial assistance.

References

1. Kelly GS. Clinical applications of *N*-acetylcysteine. Altern Med Rev 1998;3:114–27.
2. Das KC, Lewis-Molock Y, White CW. Activation of NF-κ B and elevation of MnSOD gene expression by thiol reducing agents in lung adenocarcinoma (A549) cells. Am J Physiol 1995;269:L588–602.
3. Kim KY, Rhim T, Choi I, et al. *N*-acetylcysteine induces cell cycle arrest in hepatic stellate cells through its reducing activity. J Biol Chem 2001;276:40591–8.
4. Oka S, Kamata H, Kamata K, et al. *N*-acetylcysteine suppresses TNF-induced NF-κB activation through inhibition of IκB kinases. FEBS Lett 2000;472:196–202.
5. Halliwell B, Gutteridge JMC. Free Radicals in Biology and Medicine, 3rd edition. New York: Oxford University Press Inc.; 1999. p. 936.
6. McCord JM, Fridovich I. Superoxide dismutase. An enzymic function for erythrocuprein (hemocuprein). J Biol Chem 1969;244:6049–55.
7. Bae YS, Kang SW, Seo MS, et al. Epidermal growth factor (EGF)-induced generation of hydrogen peroxide.

Role in EGF receptor-mediated tyrosine phosphorylation. J Biol Chem 1997;272:217–21.
8. Burdon RH, Rice-Evans C. Free radicals and the regulation of mammalian cell proliferation. Free Radic Res 1989;6:345–58.
9. Sundaresan M, Yu ZX, Ferrans VJ, et al. Requirement for generation of H2O2 for platelet-derived growth factor signal transduction. Science 1995;270:296–9.
10. Grana X, Reddy EP. Cell cycle control in mammalian cells: role of cyclins, cyclin-dependent kinases (CDKs), growth suppressor genes and cyclin-dependent kinase inhibitors (CKIs). Oncogene 1995;11:211–9.
11. Sherr CJ. Mammalian G_1 cyclins and cell cycle progression. Proc Assoc Am Phys 1995;107:181–6.
12. Diehl JA, Cheng M, Roussel MF, et al. Glycogen synthase kinase-3β regulates cyclin D1 proteolysis and subcellular localization. Genes Dev 1998;12:3499–511.
13. Esposito F, Cuccovillo F, Vanoni M, et al. Redox-mediated regulation of p21(waf1/cip1) expression involves a posttranscriptional mechanism and activation of the mitogen-activated protein kinase pathway. Eur J Biochem 1997;245:730–7.
14. Menon SG, Coleman MC, Walsh SA, et al. Differential susceptibility of nonmalignant human breast epithelial cells and breast cancer cells to thiol antioxidant-induced G(1)-delay. Antioxid Redox Signal 2005;7:711–8.
15. Menon SG, Sarsour EH, Spitz DR, et al. Redox regulation of the G_1 to S phase transition in the mouse embryo fibroblast cell cycle. Cancer Res 2003;63:2109–17.
16. Sarsour EH, Agarwal M, Pandita TK, et al. Manganese superoxide dismutase protects the proliferative capacity of confluent normal human fibroblasts. J Biol Chem 2005;280:18033–41.
17. Savitsky PA, Finkel T. Redox regulation of Cdc25C. J Biol Chem 2002;277:20535–40.
18. Yamauchi A, Bloom ET. Control of cell cycle progression in human natural killer cells through redox regulation of expression and phosphorylation of retinoblastoma gene product protein. Blood 1997;89:4092–9.
19. Spitz DR, Oberley LW. An assay for superoxide dismutase activity in mammalian tissue homogenates. Anal Biochem 1989;179:8–18.
20. Beers RF, Jr., Sizer IW. A spectrophotometric method for measuring the breakdown of hydrogen peroxide by catalase. J Biol Chem 1952;195:133–40.
21. Venkataraman S, Jiang X, Weydert C, et al. Manganese superoxide dismutase overexpression inhibits the growth of androgen-independent prostate cancer cells. Oncogene 2005;24:77–89.
22. Davidson BL, Allen ED, Kozarsky KF, et al. A model system for *in vivo* gene transfer into the central nervous system using an adenoviral vector. Nat Genet 1993;3:219–23.
23. Begg AC, McNally NJ, Shrieve DC, et al. A method to measure the duration of DNA synthesis and the potential doubling time from a single sample. Cytometry 1985;6:620–6.
24. Conour JE, Graham WV, Gaskins HR. A combined *in vitro*/bioinformatic investigation of redox regulatory mechanisms governing cell cycle progression. Physiol Genom 2004;18:196–205.
25. Goswami PC, Sheren J, Albee LD, et al. Cell cycle-coupled variation in topoisomerase IIα mRNA is regulated by the 3′-untranslated region. Possible role of redox-sensitive protein binding in mRNA accumulation. J Biol Chem 2000;275:38384–92.
26. Mauro F, Grasso A, Tolmach LJ. Variations in sulfhydryl, disulfide, and protein content during synchronous and asynchronous growth of HeLa cells. Biophys J 1969;9:1377–97.
27. Rapkine L. Sulphydryl groups and enzymic oxido-reduction. Biochem J 1938;32:1729–39.
28. Menon SG, Goswami PC. A redox cycle within the cell cycle: ring in the old with the new. Oncogene 2007;26:1101–9.
29. Finkel T. Reactive oxygen species and signal transduction. IUBMB Life 2001;52:3–6.
30. Bakiri L, Lallemand D, Bossy-Wetzel E, et al. Cell cycle-dependent variations in c-Jun and JunB phosphorylation: a role in the control of cyclin D1 expression. EMBO J 2000;19:2056–68.
31. Guttridge DC, Albanese C, Reuther JY, et al. NF-κB controls cell growth and differentiation through transcriptional regulation of cyclin D1. Mol Cell Biol 1999;19:5785–99.
32. Nagata D, Suzuki E, Nishimatsu H, et al. Transcriptional activation of the cyclin D1 gene is mediated by multiple *cis*-elements, including SP1 sites and a cAMP-responsive element in vascular endothelial cells. J Biol Chem 2001;276:662–9.
33. Zou Y, Ewton DZ, Deng X, et al. Mirk/dyrk1B kinase destabilizes cyclin D1 by phosphorylation at threonine 288. J Biol Chem 2004;279:27790–8.
34. Cao C, Leng Y, Huang W, et al. Glutathione peroxidase 1 is regulated by the c-Abl and Arg tyrosine kinases. J Biol Chem 2003;278:39609–14.
35. Cao C, Leng Y, Kufe D. Catalase activity is regulated by c-Abl and Arg in the oxidative stress response. J Biol Chem 2003;278:29667–75.
36. Wlodek L. Beneficial and harmful effects of thiols. Pol J Pharmacol 2002;54:215–23.

Superoxide Signaling Mediates *N*-acetyl-l-cysteine–Induced G_1 Arrest: Regulatory Role of Cyclin D1 and Manganese Superoxide Dismutase

Sarita G. Menon, Ehab H. Sarsour, Amanda L. Kalen, et al.

Cancer Res 2007;67:6392-6399.